Magazine of Concrete Research, 2000, **52**, No. 4, Aug., 303–319

Factors affecting the efficiency of repair to propped and unpropped bridge beams

P. S. Mangat* and F. J. O'Flaherty*

Sheffield Hallam University

This paper presents the results of laboratory and field investigations of bridge beams repaired both under propped and unpropped conditions. In the laboratory, beams were repaired using hand-applied repairs. Repairs to beams in two highway bridges were carried out using both hand-applied and flowing repairs. The repair materials used were commercial products of wide-ranging properties (shrinkage, creep and elastic modulus). Both low stiffness repair materials of elastic modulus, E_{rm}, less than the substrate E_{sub}, and high stiffness repair materials ($E_{rm} > E_{sub}$) were used. The repairs were applied in the tensile zone of the beams. Strain distributions in the different phases of repair patches were monitored under service loading for a period of up to 240 weeks. The results show that high structural efficiency is achieved with repairs having $E_{rm} > E_{sub}$, other properties (shrinkage and creep) being within reasonable limits. Such repairs are less prone to restrained shrinkage cracking and show a capacity for load redistribution into the repair patch. Low stiffness repairs ($E_{rm} < E_{sub}$), on the other hand, are prone to restrained shrinkage cracking and are ineffective in load-sharing with the substrate. Repairs to propped flexural members developed erratic and non-uniform load distribution in the different phases upon reapplication of load. Composite action between the repair patch and the substrate results in cracking in the repair patch, rendering the repairs structurally inefficient.

Introduction

The scale of the problem of corroding reinforced concrete highway bridges requiring repair is very great. A recent survey for the former Department of Transport, for example, has revealed over 75% of their bridge stock to be contaminated by chlorides which, in time, will cause reinforcement corrosion.[1] Many commercial repair materials are available and the selection for particular applications is based on performance data satisfying typical current standards and specifications.[2–4] The principal selection criteria have been their dimensional stability, strength and high bond strength with the substrate concrete.

The importance of the mismatch of basic material properties between the repair patch and substrate concrete such as elastic modulus, shrinkage and creep has been recognized but their effect is not taken into account in any significant quantitative manner.[5–7] Compatibility between the repair material and substrate concrete is important for prevention of cracking.[8,9] It has been recommended that the elastic modulus of a repair material should be ± 10 N/mm^2 of the substrate concrete.[10] However, optimum compatability is not necessarily achieved by equating the properties of the repair and substrate material.[11] Research on *in situ* reinforced concrete compression members of highway bridges has shown that efficient repairs are achieved when $E_{rm} > E_{sub}$, with maximum efficiency provided by $E_{rm} \simeq 1{\cdot}3E_{sub}$.[12,13] Repairs with $E_{rm} > E_{sub}$ prevent restrained shrinkage cracking and are also effective in provided long-term structural interaction with the substrate.[12,13] The properties required of a repair material to satisfy structural or cosmetic needs are quite different and may even be contradictory. For example, good resistance to cracking may be achieved by both high shrinkage and low elastic modulus combined with high

* Sheffield Hallam University, School of Environment and Development, City Campus, Pond Street, Sheffield S1 1WB, UK.

MCR 805 Paper received 28 July 1999; last revised 22 February 2000; accepted 13 April 2000.

creep of the repair material[9] whereas the long-term structural efficiency of such repairs will be very poor.[14] Similarly, the application of highly impermeable repairs may be desirable to prevent further ingress of deleterious substances in the repair patch but very low porosity would accelerate bond cracking along the reinforcement upon renewed or continuing corrosion in the repair patch.[15,16] The effectiveness of repairs in tensile zones mainly concerns corrosion protection of reinforcement. Structural contribution by stress redistribution is more effective in the compression zone of beams and in compression members. Results of structural interaction of repairs in compression members are reported in recent papers.[12–14]

The methods of repair commonly used are hand-applied, sprayed and flowing repairs.[2] The repairs may be applied to unpropped or propped structures. Recent research on compression members of bridge structures[12–14] shows that, in both propped and unpropped repairs, application of materials with $E_{rm} > E_{sub}$ results in effective shrinkage transfer to the substrate, leading to reduced risk of restrained shrinkage cracking. Such repairs are also efficient in long-term load-sharing. In repairs to propped compression members, long-term structural interactions are erratic. They are governed by the depropping process which can disturb the original load distribution (before propping) in the structure. The importance of the mechanical interaction between the substrate concrete and repair is also emphasized elsewhere.[17,18] In particular, the role of shrinkage/expansion and its influence on stress transfer is considered theoretically[17] and through field monitoring of repair to a portal frame.[18] The theoretical approach predicts that the elastic modulus and shrinkage of the repair, together with the degree of restraint exerted by the substrate, influence the magnitude of stress, but the effects of creep and shrinkage transfer by the stiffer repair to the substrate[12,14] are not considered. The field study[18] shows that deformation of the repair against the restraint provided by the substrate will ensure continued direct stress and shear stress transfer. A theoretical approach has also been developed to evaluate the ultimate strength of beams with deteriorated tensile reinforcement, before and after repair.[19]

Experimental programme

Beams incorporating repair patches were manufactured in the laboratory for testing under long-term loading. Parallel investigations on two highway bridges were undertaken. In these, bridge beams were repaired using hand-applied and flowing repairs. The repairs were applied under propped and unpropped conditions. The repair materials used were predominantly commercial products. Strain distributions in different phases of the repair patches were monitored under service loading for a period of up to 240 weeks (nearly five years).

Laboratory investigation

Details of repaired reinforced concrete beam. Eight reinforced concrete beams measuring 2740 × 100 × 200 mm were cast in steel moulds—details are given in Fig. 1. The beams were reinforced with two 16 mm diameter high-strength steel bars at a cover of 30 mm. Mild steel links 6 mm in diameter and at 110 mm spacing were provided in the shear zones and they were supported with 6 mm diameter mild steel hanger bars in the compression zone (Fig. 1(a)). To simulate a repair situation where deteriorated concrete has been removed, voids measuring 640 mm long by 71 or 96 mm deep were inserted centrally at the casting stage, as shown in Fig. 1(b). Sections through a typical beam are given in Figs 1(c) and 1(d). Before casting a beam, a block of stiff polystyrene was inserted centrally around the reinforcement cage and sealed to create the void for the repair patch.

The steel mould was lightly coated with mould oil and the reinforcement cage was positioned in the mould, care being taken not to damage the strain gauge wires from the reinforcement. Concrete was mixed dry in a pan mixer for 2 min, water was then added and mixing continued to yield a homogeneous mix. All beams were cast horizontally in three layers, each layer being compacted with a poker vibrator. The top surface of the concrete was levelled off and covered with polythene sheeting. Two 100 mm^3 cubes and two 200 × 100 mm diameter cylinders were cast simultaneously with each beam for 28-day compressive strength and elastic modulus tests. The beams remained in the mould for four days, under laboratory conditions of temperature and humidity. They were then demoulded and cured in the laboratory air to 28 days age before loading. Prior to loading, the polystyrene block was removed, leaving a void which was repaired at a later stage. The internal surfaces of the void, which formed the substrate/repair interface, were roughened by a chisel to simulate site practice for enhancing bond.

Deterioration processes in reinforced concrete structures are long-term phenomena and the need for repair normally occurs after a structure has been in service for many years. As a result, the creep and shrinkage of the substrate concrete have stabilized and reached negligible levels when repairs normally take place. In order to simulate these conditions in the laboratory, the reinforced concrete beams with the void were loaded for six to eight weeks prior to the application of repair to eliminate the effects of creep in the substrate concrete. Serviceability loads under four-point bending were applied as described in the following subsection and the loaded members were stored in a controlled environment (20°C, 55% relative humidity (RH)).

Repair of six reinforced concrete beams was then carried out while still under load (unpropped state) and two beams were repaired in a propped state, that is

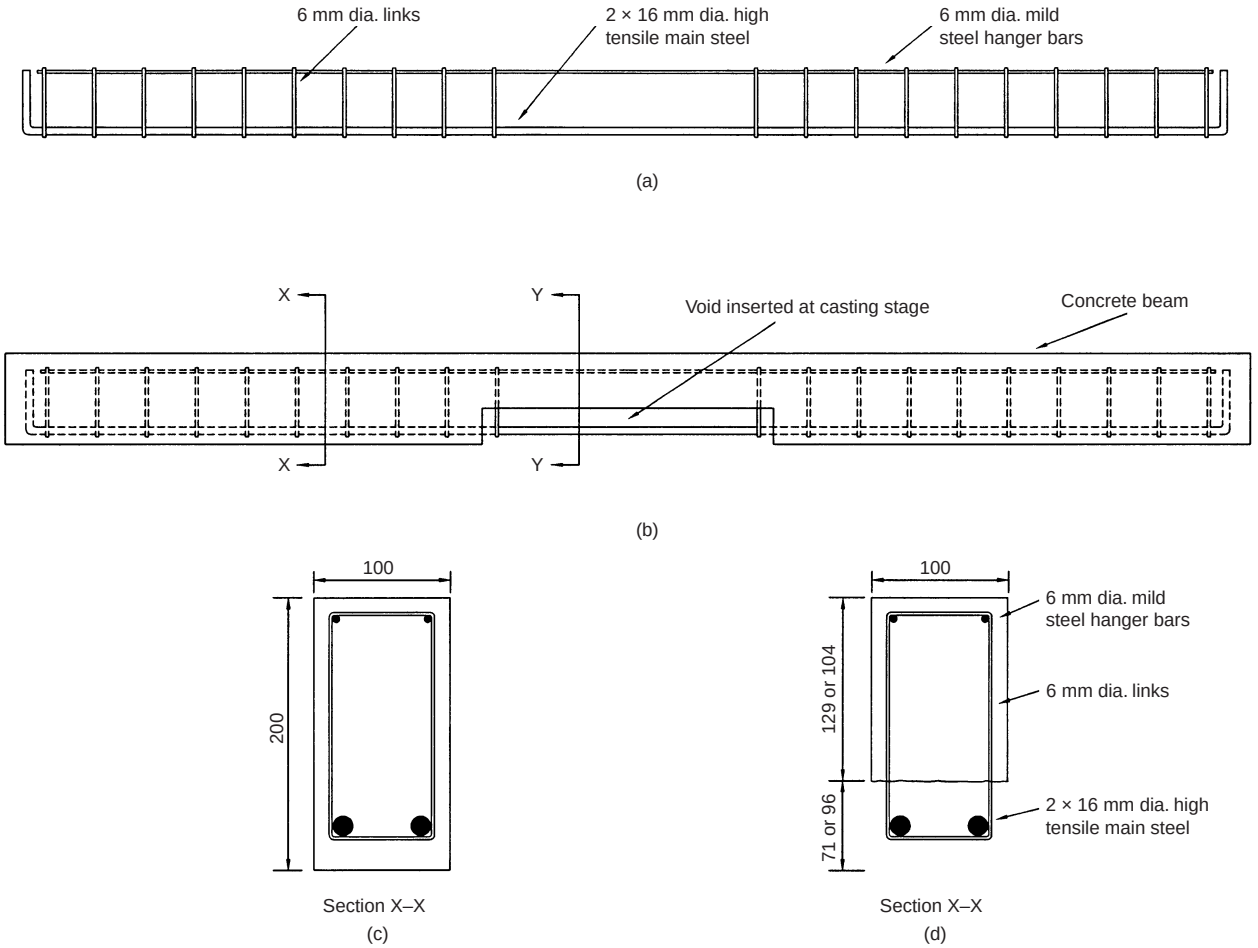

Fig. 1. Reinforced concrete (RC) beams manufactured in the laboratory: (a) steel reinforcement details; (b) RC beam with repair void; (c) cross-section of beam; and (d) cross-section through the repair void (all dimensions in mm)

unloaded (Table 1). Repairs to unpropped beams were applied by placing timber formwork on the soffit of the beam and supporting it with wedges built up from the top flange of the creep rig (see following subsection). This allowed the repair material to be inserted into the void from either side (vertical face) of the beam as shown in Fig. 2. Embedment gauges within the repair material were also inserted as the repair progressed (Fig. 2). Each repair material was mixed in accordance with the manufacturers' instructions. The material was hand-built to within 10 mm of the finished surface

Fig. 2. Application of hand-applied repair, unpropped beam

Table 1. Laboratory repairs to reinforced concrete beams

Beam	Repair material	Loading during repair	Depth of repair: mm
1	G4(L)	Unpropped	71
2	G5(L)	Unpropped	71
3	G5(L)	Unpropped	96
4	G6(L)	Unpropped	71
5	L3(L)	Unpropped	71
6	G5(L)	Propped	71
7	L3(L)	Propped	71
8	L3(L)	Unpropped	96

before a final coat was applied and smoothened with a steel float. Upon completion, the fresh repair was covered with polythene sheeting. After 24 h of curing, demec points were attached to the surface of the repair patch at a gauge length of 100 mm (see later). After three days, the polythene sheeting and formwork were removed.

Repairs were applied to two beams (Table 1) after releasing the service load (propped state). The load was

reapplied when the cube strength of the repair material reached the strength of the substrate concrete or at 28 days, whichever was sooner. The repaired beams, under load, were stored in a controlled environment (20°C, 55% RH) throughout the monitoring period.

Loading arrangement. Custom-built creep rigs, shown in Fig. 3, applied a constant serviceability load to each reinforced concrete beam (Table 1). The rig consists of a $203 \times 102 \times 23$ kg/m universal beam and a loading cross-head applying point loads at one-third span sections along the beam. A serviceability load, approximately 40% of the ultimate load (11 kN at each load point), was applied on each beam. The load was applied by a torque wrench which was calibrated to a capacity of 22 kN with an accuracy of ±3%. The calibration was rechecked frequently during the test programme. The applied load was maintained at constant level by tightening the loading bolt in the top platen of the rig (Fig. 3). The load was topped up at regular intervals to maintain the constant value of 11 kN at each load point.

Strain monitoring. One CEA-06-250 UN-120 electrical resistance strain gauge, supplied by Micro Measurements Group, was attached at mid-span to one tensile reinforcing bar in each beam at the location shown in Fig. 4 (steel 1). Three PML 30 electrical resistance gauges, supplied by Tokyo Sokki Kenkyujo Co., were embedded in the repair material during the application of repair at locations RM1, 2 and 3 shown in Fig. 4. All gauges were located at mid-span along the longitudinal centre of the section. Gauge RM1 was at the repair/substrate interface, RM2 was at reinforcement level and RM3 was at the soffit. All gauges were connected to a ten-channel digital strain indicator for continuous monitoring. The gauge length was 40 mm. Surface strains were also monitored at locations Dem 1, Dem 2 and Dem 3, shown in Fig. 4, by demec gauges of 100 mm gauge length. The strains monitored on the opposite faces, at a common distance from the soffit, were averaged.

Materials. A concrete mix of proportions (by weight) of 1:1·8:2·9 with a water/binder of 0·45 was used. The binder content was 340 kg/m^3 of ordinary Portland cement plus 60 kg/m^3 of pulverized fuel ash. Details and properties of the substrate concrete and repair materials are given in Table 2. All repair materials are commercial products. Material G4 is a heavy duty repair mortar containing styrene acrylic copolymer and admixtures including a waterproofing agent, ordinary Portland cement, fibres, 6 mm down-graded aggregate and 10 mm size granite aggregate. Material G5 contains finely ground Portland cement with some sulphoaluminate cement, microsilica, fibres, other pozzolanic materials and styrene acrylic

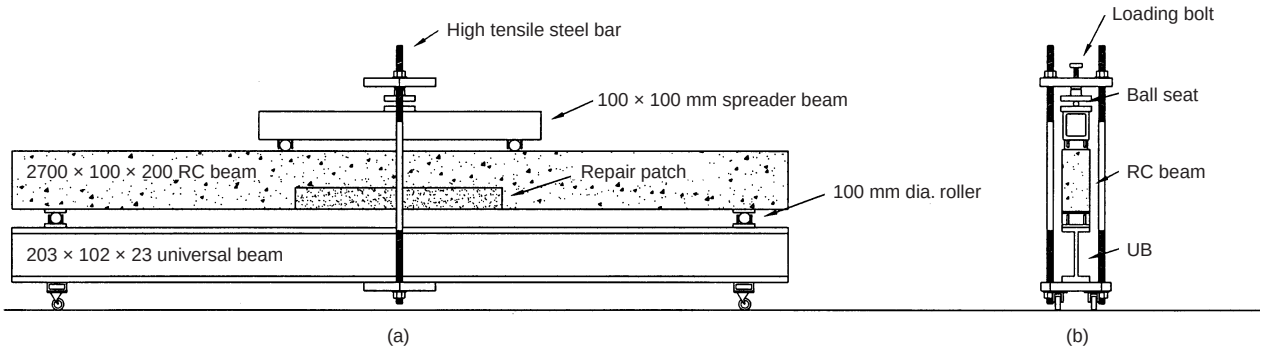

Fig. 3. Repaired reinforced concrete beam under sustained loading: (a) elevation; and (b) end view

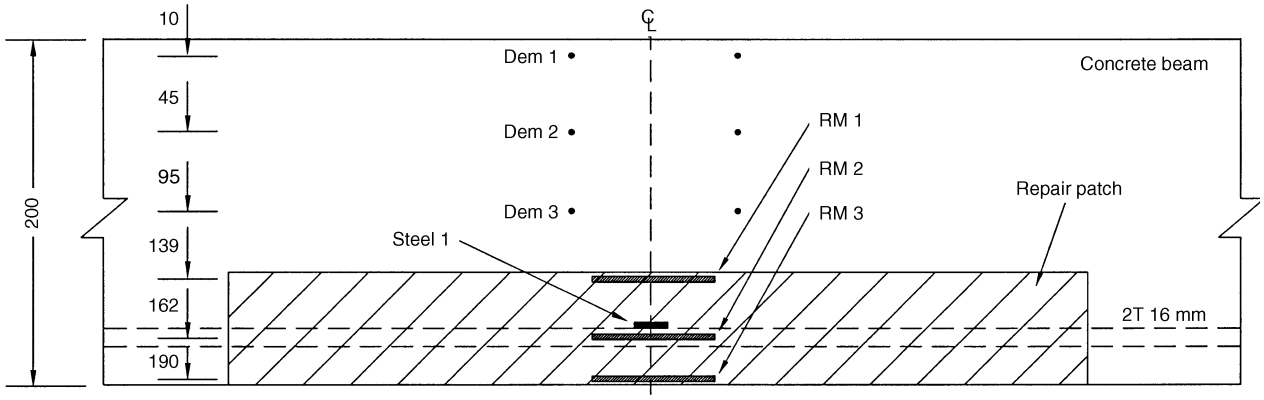

Fig. 4. Location of strain gauges in the repair patch of the laboratory beams (all dimensions in mm)

Table 2. Details of substrate concrete and repair materials

Site	Material	Comp. strength: N/mm^2	Elastic modulus: kN/mm^2	E_{rm}/E_{sub}	Shrinkage/ expansion* (100 days) μstrain	Creep* (70 days) μstrain	Mod. of rupture (21 months): N/mm^2
Laboratory	G4(L)	46	24·0	1·17	401 (184)	745	8·8
	G5(L)	50	19·6	0·96	1087 (539)	1411	4·7
	G6(L)	31	11·5	0·56	1100 (565)	1188	3·3
	L3(L)	35	27·4	1·34	710 (640)	748	1·9
	Concrete substrate	45	20·5	—	—	—	—
Gunthorpe bridge	G4	46	24·0	0·85	401 (184)	745	8·8
	G5	50	19·6	0·7	1087 (539)	1411	4·7
	G6	31	11·5	0·41	1100 (565)	1188	3·3
	Concrete substrate	—	28·1	—	—	—	—
Sutherland Street bridge	S1	79	24·2	1·04	740 (350)	445	6·5†
	S3	68	31·9	1·38	791 (286)	667	5·7
	S4	39	27·4	1·18	388 (285)	454	4·3
	Concrete substrate	—	23·2	—	—	—	—

* Shrinkage and creep under 20°C, 55% RH exposure, expansion in water-cured specimens (values given in brackets).
† At 14 months age.

copolymer. Material G6 is a rapid hardening mortar incorporating advanced cement chemistry, microsilica, fibre and styrene acrylic copolymer. Material L3 is a general purpose repair mortar. It contains Portland cement, graded aggregates, special fillers and chemical additives to control shrinkage and minimize water demand. Each material is suitable for application by hand. Material L3 has also been used for dry spray application.[12]

Gunthorpe bridge

Details of repaired beams. Gunthorpe bridge is a three-span reinforced concrete arch bridge across the River Trent at Gunthorpe, Nottinghamshire. It comprises a central arch and two side arches. Each of the arches contains four ribs. The bridge deck is supported by lateral beams spanning the arch ribs as shown in Fig. 5. Repairs were carried out to typical corroding beams spanning between the arch ribs on

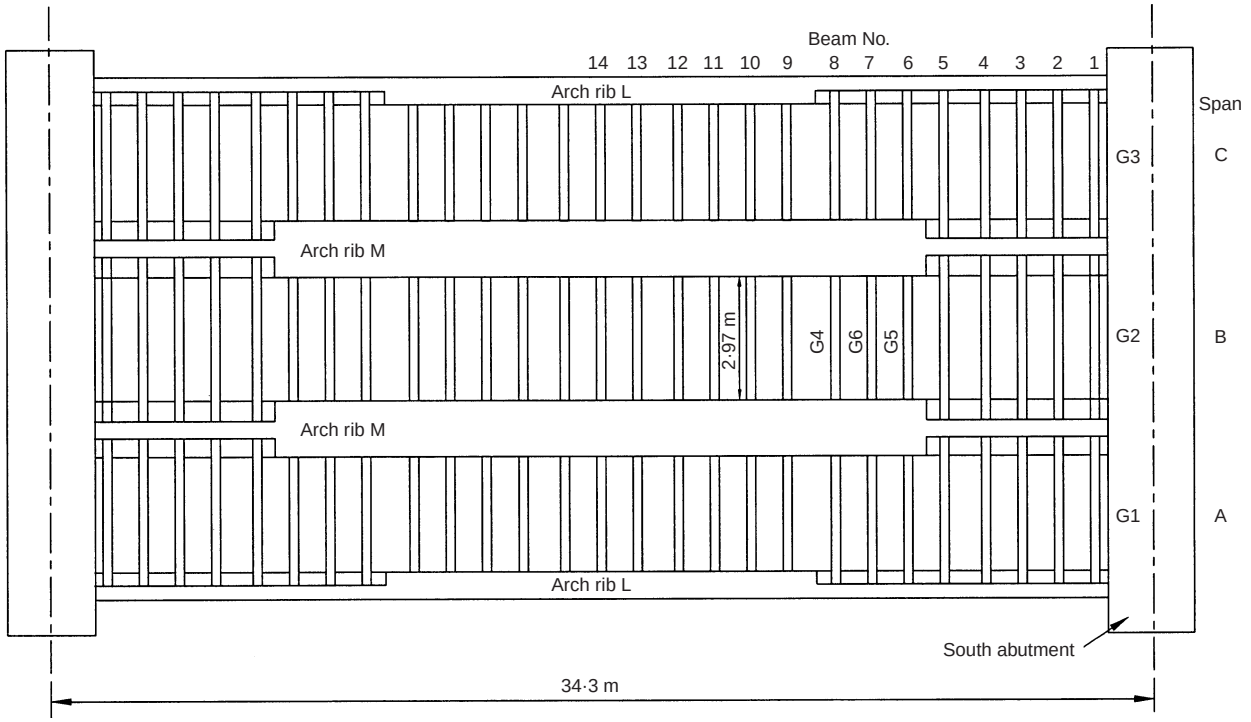

Fig. 5. South span of Gunthorpe bridge showing the lateral beams spanning the arch ribs

the south span of the bridge. Results of beams B6, B7 and B8 (repaired with materials G5, G6 and G4 respectively), which were located under the main carriageway of the bridge, are given in this paper.

Instrumentation. The lateral beams were instrumented with vibrating wire strain gauges after repair. At the mid-span of each beam, four surface gauges were installed along the web (vertical face) of the beam (Fig. 6). One of the gauges also monitored the atmospheric temperature. Two of the surface gauges were positioned at the substrate/repair interface. A fifth strain gauge was positioned on the soffit to monitor extreme fibre strains. The steel reinforcement strain was measured on one reinforcing bar, at mid-span, by means of a vibrating wire gauge. All the gauge cables were carried via uPVc trunking to a central logging system where the gauges were automatically scanned at regular intervals.

Materials and methods of repair. Beams B6, B7 and B8 (Fig. 5) were repaired in an unpropped state (no temporary support). Deteriorated concrete was removed along the full length of each beam to a depth of about 25 mm behind the steel. The total depth of the repair patch was 120–130 mm (Fig. 6). The repair materials were mixed on site in a barrel mixer. They were then applied by hand to a depth of about 10 mm from the finished surface. The final coat was applied a few hours later when the material had set slightly. The finished surface was obtained by levelling with a wooden float and screeding with a damp sponge. Hand-applied repair materials G4, G5 and G6 were used at Gunthorpe bridge. The properties of the substrate concrete and the repair materials are given in Table 2. These repair materials were also used in the laboratory investigation and are represented by suffix (L) in Table 2.

Sutherland Street bridge

Details of repaired beams. The substructure (Fig. 7) of Sutherland Street bridge, on the B6080 in Sheffield, consists of reinforced concrete beams and columns in a portal frame configuration. The structure was in a state of deterioration due to reinforcement corrosion. Repairs were applied to the central span of the beams in each portal frame, as shown in Fig. 7, using flowing materials.

Instrumentation. Vibrating wire strain gauges were used to monitor strains in the repair patches. The location of gauges is shown in Fig. 8. Two vibrating wire gauges were embedded in the repair patch, one being attached to the substrate at the interface with the repair (labelled 'subs') and the other to the longitudinal steel (labelled 'steel'). The cables of all gauges were carried through 50 mm uPVC trunking to a central data logger (Fig. 7, south frame) which automatically scanned the gauges regularly.

Materials and methods of repair. The portal frame beams at Sutherland Street bridge were repaired in a propped state. The south frame and half of the north frame of the bridge were propped (Fig. 7). Every second beam of the bridge deck was propped with steel props designed by Mabey Support Systems Ltd.

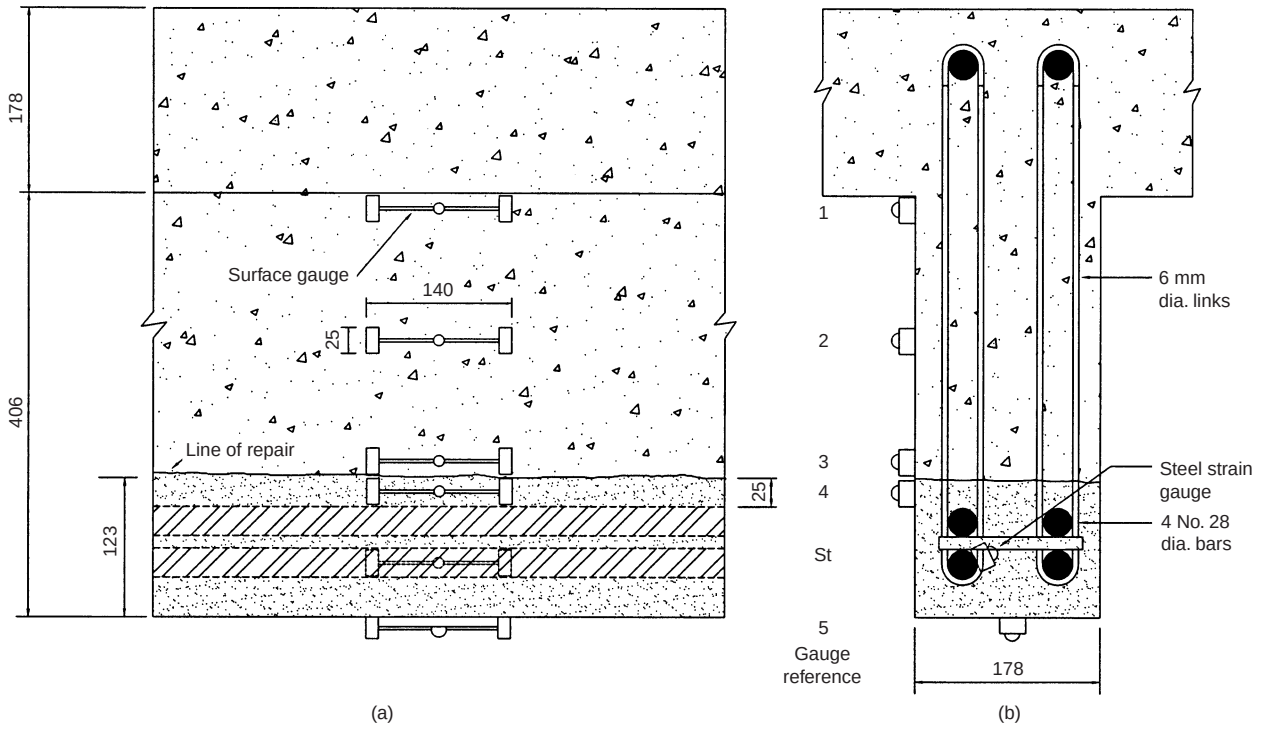

Fig. 6. Section details of lateral beams at Gunthorpe bridge, with location of gauges: (a) elevation; and (b) cross-section (all dimensions in mm)

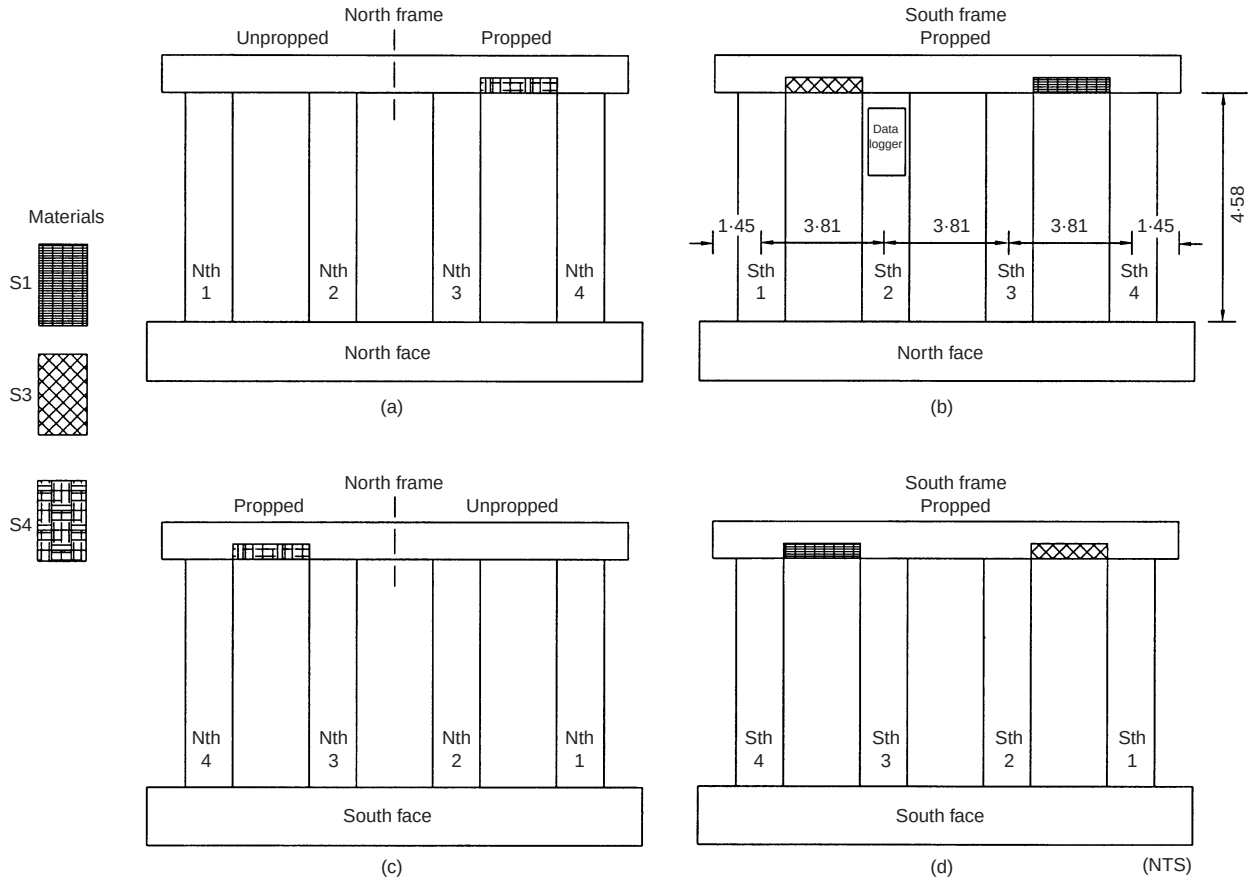

Fig. 7. Substructure of Sutherland Street bridge showing locations of beam repair: (a) North face of north frame (half unpropped, half propped); (b) north face of south frame (propped); (c) south face of north frame (half propped, half unpropped); and (c) south face of south frame (propped) (all dimensions in m)

The deteriorated concrete was removed by both water-jetting and mechanical means to a depth of 25 mm behind the steel. Plywood-faced timber formwork was used for watertight shuttering of flowing repairs. The substrate concrete was saturated by filling the shuttering with water and leaving in place overnight. The repair materials were mixed in accordance with manufacturers' instructions in a barrel mixer. They were either pumped or poured into the shuttering from a bucket. Compaction of the flowing repair was provided by firmly tapping the shuttering with a hammer at regular frequency. Shuttering was left in place for at least three days after the pour. Upon removal, any poor surface finishes received a thin coating of cementitious material. Propping remained in place until the repair materials reached the design strength of the substrate concrete or for 28 days.

Properties of the flowing repair materials applied at Sutherland Street bridge are given in Table 2. Material S1 is a cementitious material containing 5 mm maximum size graded aggregate, additives and shrinkage compensating agents. Material S3 is a rapid hardening material incorporating microsilica, shrinkage compensating admixtures, styrene acrylic copolymer and 6 mm size aggregate. Material S4 is a conventional flowing concrete containing Portland cement, 10 mm size rounded aggregate, grade M sand, pulverized fuel ash, superplasticizer and polypropylene fibres. The water: binder ratio is 0·48 and the flow >500 mm.

Results and discussion

Unpropped repairs

Laboratory tests on six beams together with the three lateral beams repaired at Gunthorpe bridge are discussed in this section. The repairs were applied to the beams in an unpropped state.

Laboratory tests, $E_{rm} > E_{sub}$. The typical strain–time relationships for beams repaired with materials G4(L) and L3(L) are plotted in Figs 9 and 10 respectively; $E_{\mathrm{rm}} = 1{\cdot}17E_{\mathrm{sub}}$ for G4(L) and $E_{\mathrm{rm}} = 1{\cdot}34E_{\mathrm{sub}}$ for L3(L) (Table 2). Datum readings of strain were taken 24 h after the application of the repair patch (represented by week 0 in Figs 9 and 10). Residual strains in the substrate concrete (gauges Dem 1, 2, 3) and steel reinforcement (gauge steel 1) were present at week 0 since the beam had been loaded at week −6 (28 days after casting) to eliminate the effects of creep in the substrate concrete (see earlier section). The 28-day curing period between casting and loading

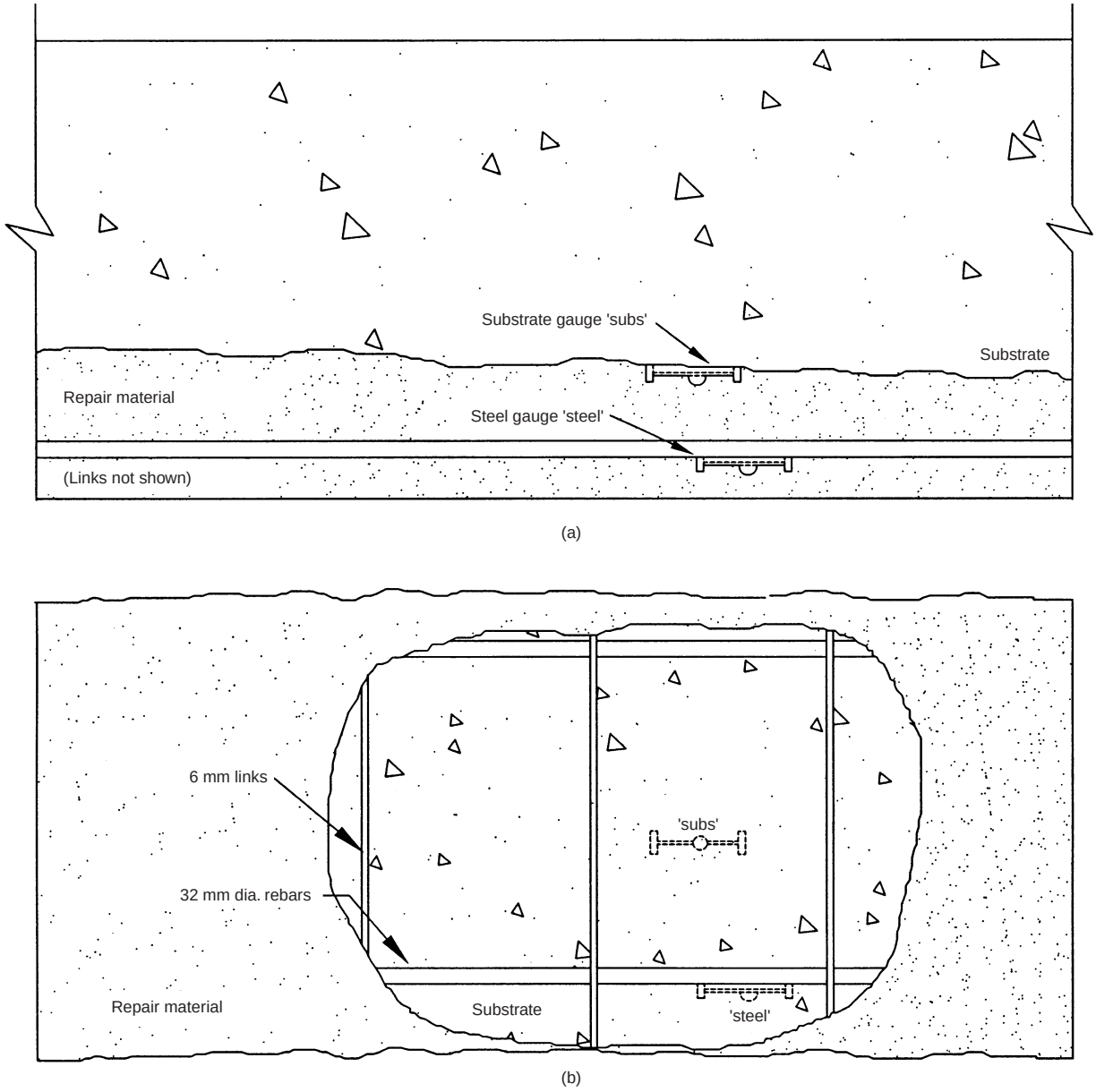

Fig. 8. Location of strain gauges in the repair patch (portal frame beams, Sutherland Street bridge): (a) elevation of beam section; and (b) internal view from soffit

is shown as weeks −10 to −6 in Figs 9 and 10.

In Figs 9 and 10, the repair material shows slight contraction (positive strain) in the early stages from week 0 to week 5 (see gauges RM1, RM2 and RM3). The contraction is least in gauge RM1 compared with RM2 and RM3. This reflects maximum restraint to the free shrinkage of the repair patch at the substrate interface (location of gauge RM1). The substrate restraint decreases with increasing distance from the interface (locations RM2 and RM3) thereby permitting greater free shrinkage and, therefore, higher compressive strain. From week 5 onwards, the tensile strains in the repair material gradually increase (gauges RM1, RM2 and RM3 in Figs 9 and 10).

The tensile strain in the steel reinforcement simultaneously decreases during this period (see gauge steel 1, Figs 9 and 10). For example, in Fig. 9, the steel strain of 666 microstrain decreases to 369 microstrain at week 50. The steel reinforcement is clearly shedding tensile load to the repair material. The tensile strains monitored by gauges RM1 and RM2 in Fig. 9 approach 1300 microstrain towards the end of the monitoring period. No visual cracking was apparent in the repair patch. Cracking would have been prevented by a number of factors

(*a*) E_{rm} being greater than E_{sub} (Table 2) enables shrinkage transfer of the repair material to the substrate at the interface[12]
(*b*) repair material G4 having low drying shrinkage and the highest modulus of rupture (Table 2) and
(*c*) a moderate degree of creep (Table 2) which results

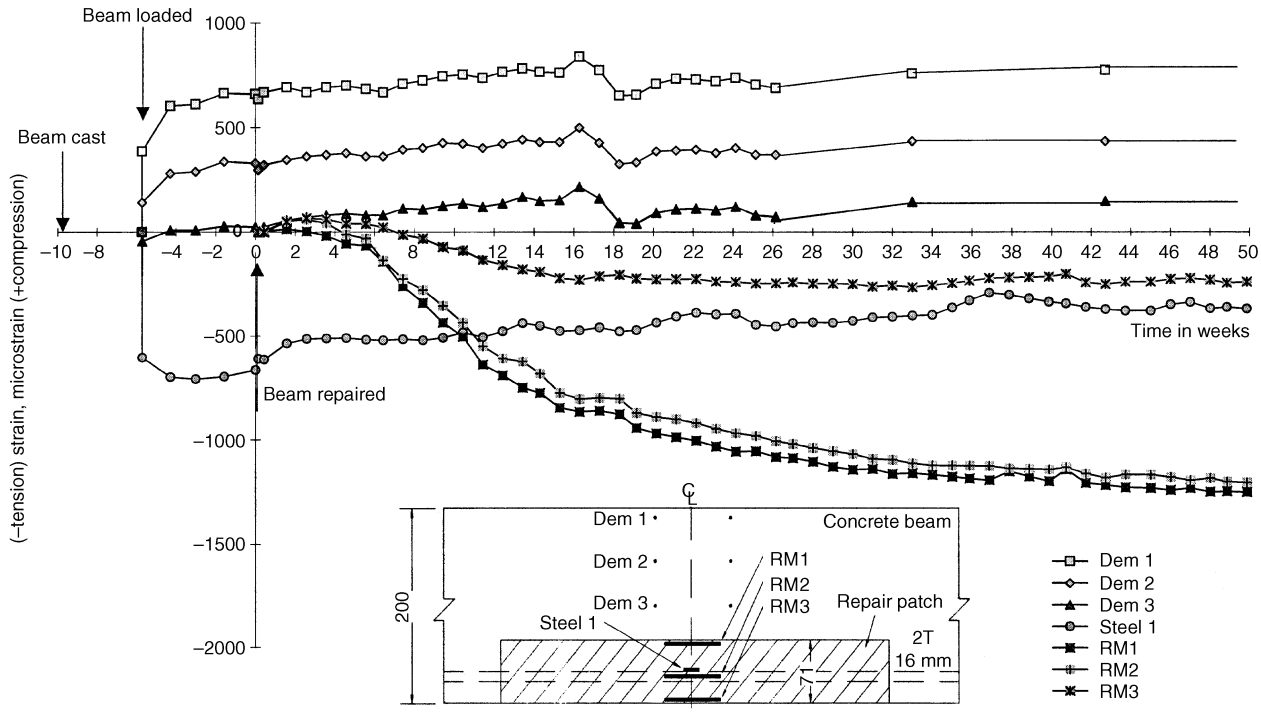

Fig. 9. Strain profiles in the beam repaired with material G4(L), $E_{rm} > E_{sub}$, unpropped repair

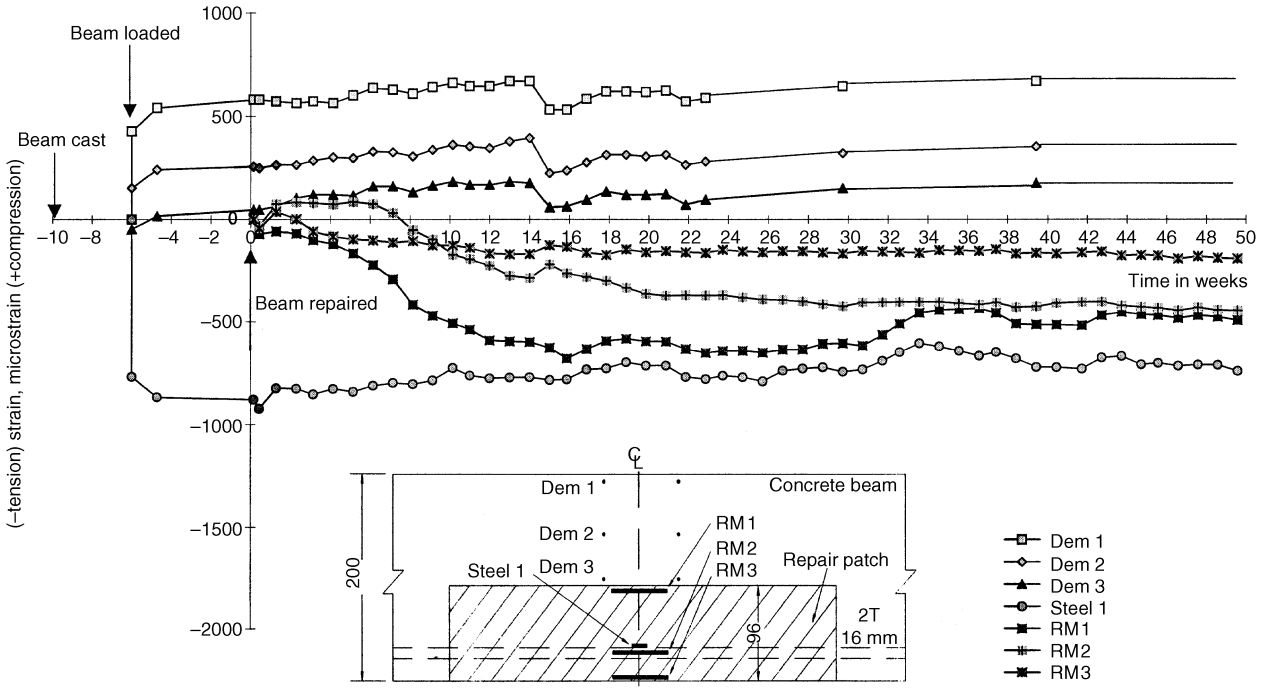

Fig. 10. Strain profiles in the beam repaired with material L3(L), $E_{rm} > E_{sub}$, unpropped repair

in some relaxation of tensile stress in the repair patch.

In the case of high stiffness ($E_{rm} > E_{sub}$) repair material L3(L) in Fig. 10, gauge RM1 at the repair/substrate interface goes into tension soon after the application of repair and develops a tensile strain of 680 microstrain after 16 weeks. The strain in gauges RM2 and RM3 changes from compression to tension at week 8 and 2 respectively. Two tensile cracks of widths less than 0·1 mm occurred in the repair patch despite the material being of high stiffness ($E_{rm} > E_{sub}$) and, therefore, being capable of transferring shrinkage stress to the substrate and reducing restrained shrinkage tension.[12] This is due to the high shrinkage of material L3(L) (relative to material G4, Table 2) and its extre-

mely low modulus of rupture, while the creep of the two materials is similar.

Figure 9 shows that the reduction in tensile strain in the steel reinforcement (gauge 'steel 1') in the repair patch of material G4(L) was 297 microstrain over the 50-week monitoring period (weeks 0–50). The reduction in steel tensile strain in the repair patch of material L3(L) was 138 microstrain (Fig. 10). This indicates a stress transfer of 62 and 29 N/mm^2 respectively from the steel reinforcement. The redistribution is more effective in material G4(L) due to the absence of cracking.

The strain in the compression zone of the beams in Figs 9 and 10 (gauges Dem 1, Dem 2 and Dem 3) remains fairly constant during the monitoring period. A drop in strain between weeks 16 and 20 is due to a temporary operational fault in the environment-controlled room which maintained 20°C, 55% RH conditions. These strain profiles indicate that the compression zone of the substrate remains fairly stable and redistribution taking place in the repair patch (in the tensile zone) has negligible effect on the compression zone.

Laboratory tests, $E_{rm} < E_{sub}$. Material G6(L) has $E_{\mathrm{rm}} = 0{\cdot}56E_{\mathrm{sub}}$ (Table 2). Strain profiles for the beam repaired with material G6(L) are plotted in Fig. 11. In the weeks immediately after the application of repair (weeks 0–5), gauges RM2 and RM3 show increasing compressive strains due to the high shrinkage of the repair material (Table 2). The compressive strain is negligible in gauge RM1 since it is attached to the repair material adjacent to the high stiffness substrate concrete ($E_{\mathrm{rm}} \ll E_{\mathrm{sub}}$), which restrains its shrinkage effectively. The restraint to shrinkage decreases as the distance from the repair/substrate interface increases. Consequently, the shrinkage strains at gauge RM3 are much higher than gauge RM2 which in turn are much higher than gauge RM1. The compressive strains measured at gauges RM2 and RM3 in Fig. 11 (material G6(L)) are much higher than corresponding values recorded in Figs 9 and 10 for materials G4(L) and L3(L). This is due to the much higher free shrinkage of material G6(L) compared with the other two materials (Table 2). The virtual tensile strain in the repair material G6(L) at this stage (week 0–5) will be its free shrinkage (1100 microstrain) minus the strain reading in the gauge (RM1, RM2 or RM3). As material G6(L) has a relatively high creep (Table 2), significant relaxation would occur, thereby reducing the tensile stress in the repair patch (week 0–5). At week 5, the compressive strains abruptly change to tensile (see RM1, RM2 and RM3, Fig. 11). This is due to cracking occurring in the material, as the tensile strain due to shrinkage restraint exceeds the tensile strain capacity of the repair material. Three cracks of width less than 0·1 mm were observed in the repair patch due to a combination of low stiffness ($E_{\mathrm{rm}} < E_{\mathrm{sub}}$), and high shrinkage.

The strain in the steel reinforcement (gauge steel 1, Fig. 11) remains fairly constant from the time of repair, as the low stiffness ($E_{\mathrm{rm}} < E_{\mathrm{sub}}$) and cracked repair material is unable to attract stress from the steel reinforcement. The strains on the substrate concrete (Dem 1, Dem 2 and Dem 3) remain constant with time throughout. It can be concluded that a repair material with $E_{\mathrm{rm}} < E_{\mathrm{sub}}$ provides inefficient repair, since it is

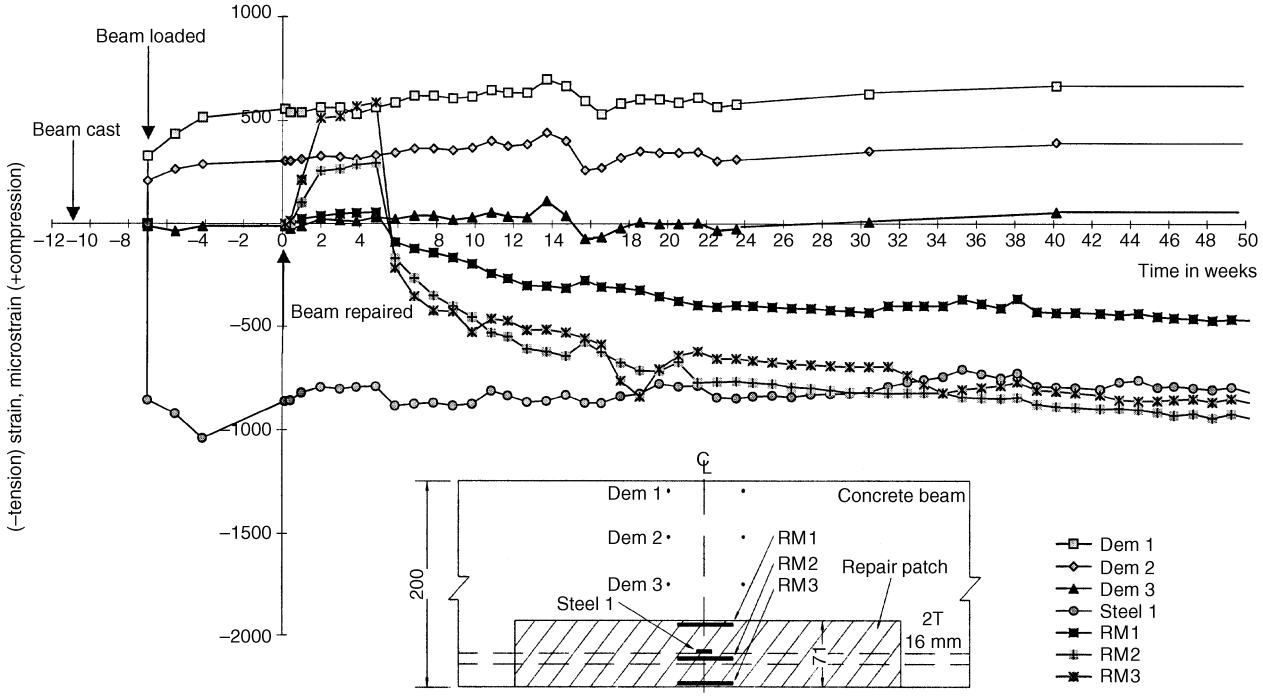

Fig. 11. Strain profiles in the beam repaired with material G6(L), $E_{rm} \ll E_{sub}$, unpropped repair

unable to attract load from the steel reinforcement and it cracks due to restraint provided by the stiffer substrate. Very high shrinkage aggravates cracking which results in even less stress redistribution from the steel reinforcement to the repair patch.

The strain profiles of the beam repaired with material G5(L), in the unpropped state, are plotted in Fig. 12; $E_{rm} = 0{\cdot}96E_{sub}$ for material G5 (Table 2). The strain profiles from gauges Dem 1, Dem 2, Dem 3 and steel 1 are very similar in both Figs 11 and 12. Observations from gauge RM3 in Fig. 12 show a sudden increase in positive strain soon after repair. This is due to observed cracking out with the gauge length of RM3. The shrinkage of material G5(L) is very high (Table 2), which is responsible for cracking and, therefore, the high positive strains of gauge RM3.

The strains monitored at gauge RM2 are consistently lower than at RM3 due to partial shrinkage restraint provided by the steel reinforcement. The shrinkage restraint provided by the substrate concrete at the repair interface (gauge RM1) is not as high as in Fig. 11 (material G6). This is due to the higher elastic modulus of material G5 than material G6, which results in substrate restraint being greater for G6.

Repairs to beams in the laboratory were carried out at relatively young age (after four weeks of curing plus six to eight weeks under load, see earlier section) compared with field structures which normally undergo repair after many years when the substrate has stabilized. The test results reported in Figs 9–12 may have, therefore, been influenced to an unknown extent by continuous hardening, shrinkage and creep (including relaxation) effects of the substrate. These effects, however, are considered to be small as explained in the following discussion. The maximum compressive strain in the substrate concrete (gauge Dem 1) upon loading, in Figs 9–12, does not exceed 400 microstrain. The resulting average stress in the compression zone of the beam, considering the neutral axis to be in the vicinity of gauge Dem 3 (Figs 9–12), approximates 4·5 N/mm^2. This represents a stress/strength of about 10%. The long-term creep strains in the substrate (gauges Dem 1 and 2) are expected to be relatively small at such a low stress: strength ratio—Figs 9–12 show that after the application of repair, long-term strains monitored from gauges Dem 1 and 2 remain fairly constant, thereby confirming small creep effects in the substrate. As far as the effects of relative properties of the repair and substrate are concerned, the key time period for these to occur is the few weeks taken by commercial repair formulations to attain their elastic modulus which mobilizes interaction with the substrate and restraint at the interface. The changes in the creep and shrinkage strains of the relatively older substrate during this short period are insignificant. Restrained shrinkage cracking within the repair patch normally occurs during this short period if sufficiently large differential shrinkage strains are developed in the repair material without sufficient relief provided by tensile creep. The longer term hardening, shrinkage and creep effects of the substrate are of little significance to this process.

Field trials, Gunthorpe bridge ($E_{rm} < E_{sub}$). The strain profiles of bridge beams repaired with materials G4 ($E_{rm}/E_{sub} = 0{\cdot}85$), G5 ($E_{rm}/E_{sub} = 0{\cdot}70$) and G6 ($E_{rm}/E_{sub} = 0{\cdot}41$) are plotted in Figs 13, 14 and 15 respectively. An immediate observation from these

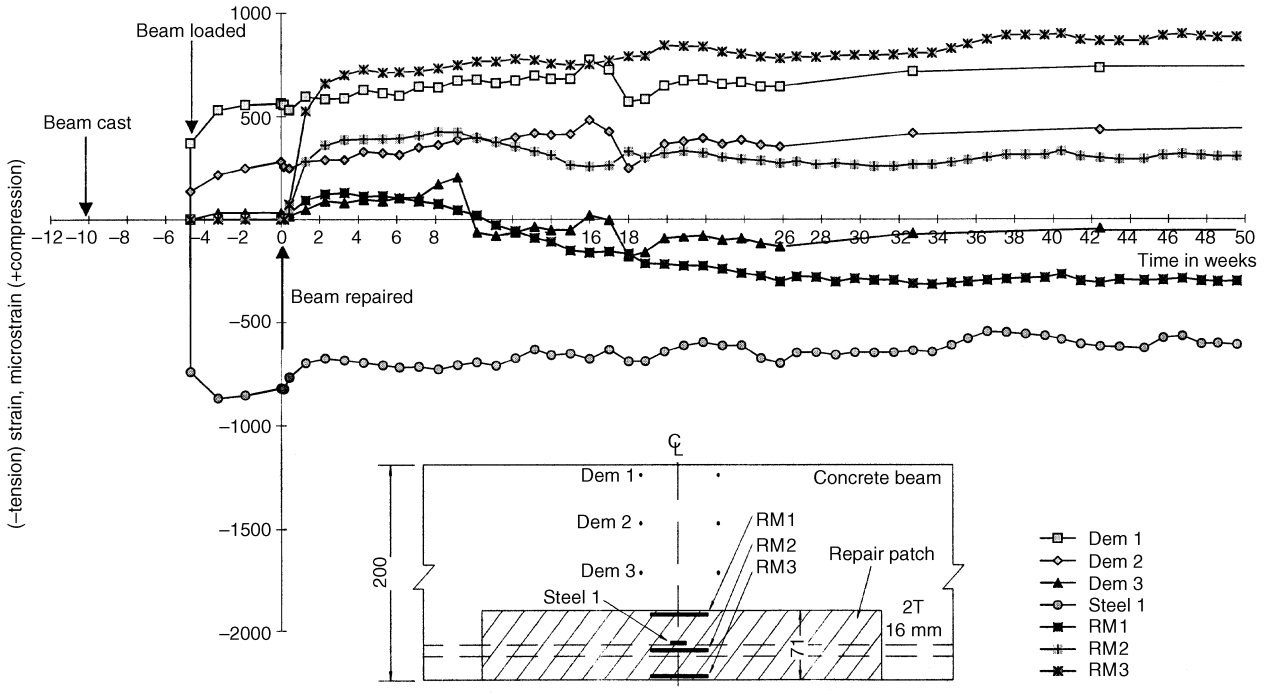

Fig. 12. Strain profiles in the beam repaired with material G5(L), $E_{rm} < E_{sub}$, unpropped repair

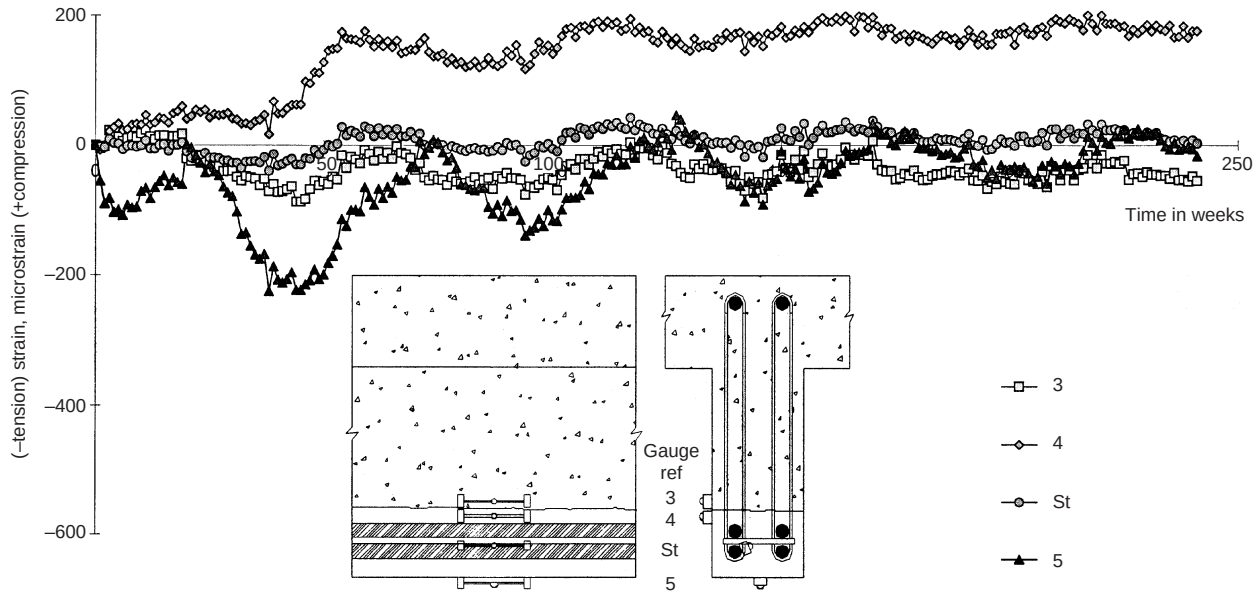

Fig. 13. Strain profiles in the lateral beam section repaired with material G4, Gunthorpe bridge, $E_{rm} < E_{sub}$, unpropped repair

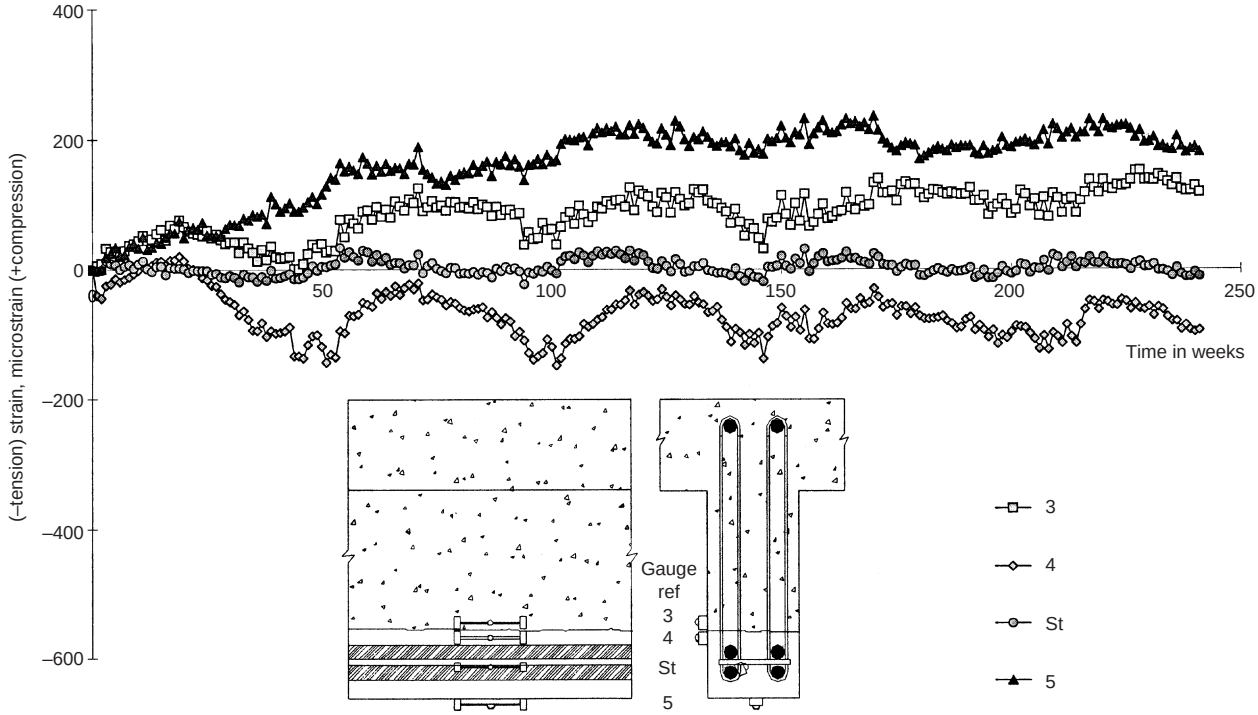

Fig. 14. Strain profiles in the lateral beam section repaired with material G5, Gunthorpe bridge, $E_{rm} \ll E_{sub}$, unpropped repair

strain profiles is their sinusoidal cyclic nature over 52-week periods. These cycles represent the annual seasonal (temperature) effects which change the strains in the concrete thermal mass.

The repair patch of material G4 in beam B8 (Fig. 13) shows fairly good strain compatibility between the substrate and repair material at the interface (gauges 3 and 4 respectively) over the first 20 weeks (approximately). The stiffness of the repair material is slightly less than that of the substrate ($E_{\mathrm{rm}}/E_{\mathrm{sub}} = 0{\cdot}85$) and the substrate is effective in restraining the shrinkage of the repair material. Over a period of time, however, the restraint to shrinkage becomes less and the strains monitored by gauges 3 and 4 drift apart. The repair material adjacent to the substrate (gauge 4) is able to attain shrinkage strains of around 200 microstrain which is about 50% of the free shrinkage of the repair material (Table 2). No tensile cracking due to restrained shrinkage was observed in the repair patch of beam B8 (Fig. 13). This was due to the relatively low free

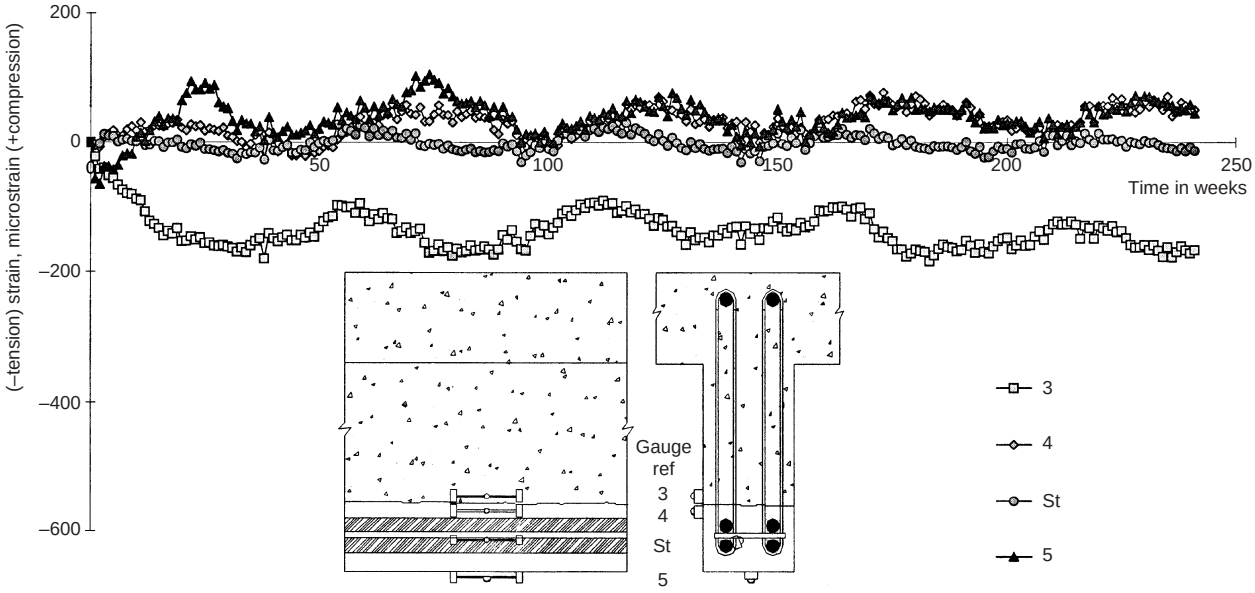

Fig. 15. Strain profiles in the lateral beam section repaired with material G6, Gunthorpe bridge, $E_{rm} \ll E_{sub}$, unpropped repair

shrinkage of material G4 and the fact that E_{rm} was only marginally less than E_{sub}, which resulted in less than absolute shrinkage restraint by the substrate.

The stiffness of the repair materials G5 and G6 used to repair beams B6 and B7 (Figs 14 and 15) was much less than the substrate ($E_{rm}/E_{sub} = 0{\cdot}70$ and $0{\cdot}41$ respectively). In addition, the free shrinkage of these repair materials was very high (Table 2). Soon after the application of repair, the substrate provided effective restraint at the interface and, therefore, caused typical restrained shrinkage cracking in the repair due to high tensile stresses. The corresponding high creep of materials G5 and G6 (Table 2) was unable to prevent cracking by relieving tensile stress. Cracking results in inconsistent strain differentials between gauges 3, 4 and 5 in Figs 14 and 15.

The strain–time profile of the steel reinforcement in Figs 13, 14 and 15 remains unaffected by the application of the repair patch. This indicates that repairs with $E_{rm} < E_{sub}$ are ineffective in causing long-term load redistribution from the reinforcement.

Propped repairs

Results of long-term laboratory tests on two beams repaired in a propped state together with beams of the portal frame at Sutherland Street bridge repaired with flowing materials are discussed in this section.

Laboratory tests ($E_{rm} > E_{sub}$). The strain–time graphs of the beam repaired with material L3(L) are plotted in Fig. 16. Datum readings were taken 24 h after the application of the repair patch (represented as week 0 in Fig. 16). Residual strains in the substrate concrete (gauges Dem 1, 2, 3) and steel reinforcement (gauge steel 1) were present at week 0, since the beam had been loaded at approximately week −9 to eliminate the effects of creep in the substrate concrete, as described earlier. The beams were cured for four weeks prior to loading, shown as approximately weeks −9 to −13 in Fig. 16. Upon unloading the beam at week 0 (simulating propping), it is observed that some compressive strain remains in the substrate concrete (gauges Dem 1 and Dem 2, weeks 0–4) due to residual creep. A small tensile strain is also evident in the steel reinforcement at week 0, but this decreases towards zero at week 4 as the free shrinkage strain of the repair patch is transferred to the steel reinforcement while the beam remains in a propped state. During the propped repair period (week 0–4), gauges RM2 and RM3 record gradually increasing compressive strains due to the free shrinkage of the repair patch. The strains recorded by gauge RM1 at the interface are very small due to restraint provided by the substrate to the early age shrinkage of the repair material.

Upon reapplication of the load at week 4, gauges Dem 1 and Dem 2 attain high compressive strains which remain relatively constant for the remainder of the monitoring period. Tensile strain is induced in the steel reinforcement (gauge steel 1) which remains relatively constant throughout the monitoring period. Negligible redistribution of strain took place in this repair patch as indicated by the almost constant strains in the steel reinforcement (gauge steel 1) and repair material (gauges RM2 and RM3). The lack of redistribution was due to severe cracking which occurred in the repair material during the reloading operation at week 4 (indicated by the sudden large tensile strain in gauges RM1 and RM2, Fig. 16). Some of the crack widths were greater than 0·1 mm. Comparing the performance of this repair patch with a similar repair patch applied to an unpropped member (Fig. 10), it is clear that propping during the application of repair and subse-

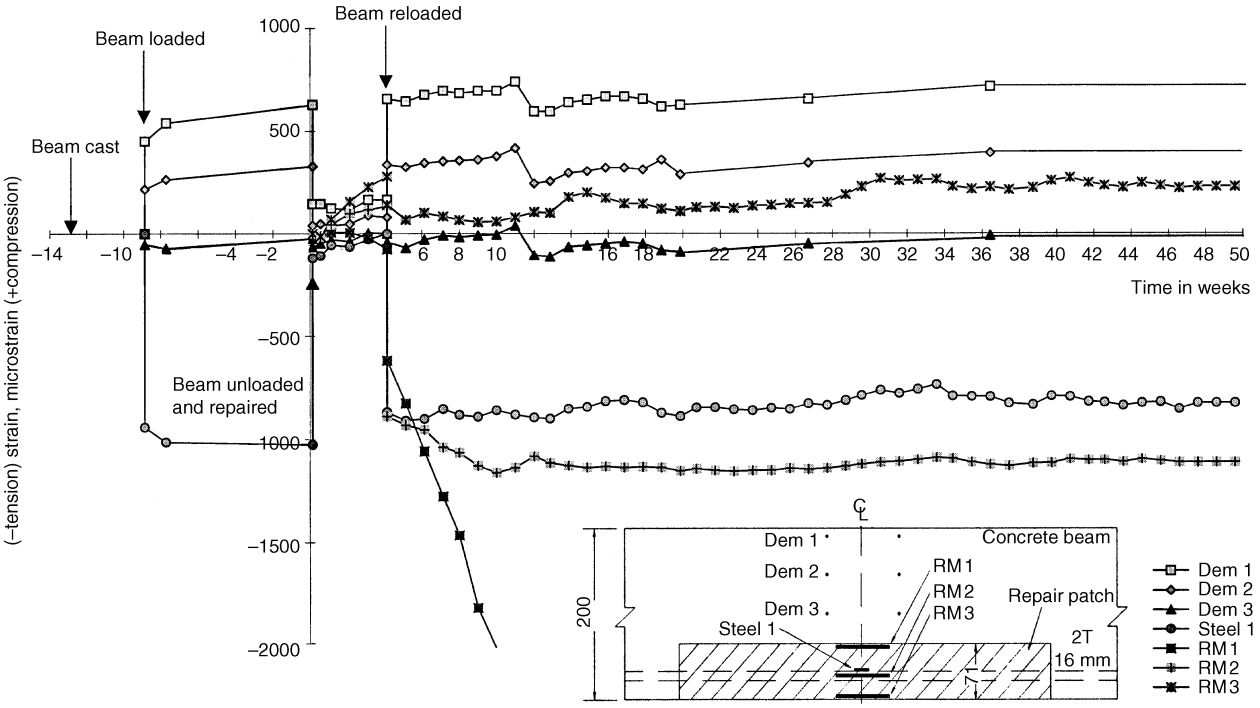

Fig. 16. Strain profiles in the beam repaired with material L3(L), $E_{rm} > E_{sub}$, propped repair

quent reloading (depropping) greatly increases the tensile strains in the repair patch (compare gauges RM2 in Figs 10 and 16). The unpropped repair with material L3(L) (Fig. 10) developed insignificant cracking compared with cracking produced in the propped repair (Fig. 16). In the case of unpropped repairs, cracking in the repair patch is caused by restrained shrinkage effects which occur gradually over a period of time and are neutralized to some extent by creep[13] and by the high stiffness ($E_{rm} > E_{sub}$) of a repair material.[14] In propped repairs, cracking is caused by the sudden load sharing (composite action) induced by depropping, which leads to typical flexural cracking in the repair patch.

Field repairs, Sutherland Street bridge ($E_{rm} > E_{sub}$). The strain–time graphs for repair patches made with flowing materials S1 and S4 are presented in Figs 17 and 18 respectively. The location of the strain gauges in the repair material at the substrate interface ('subs') and on the steel reinforcement was outlined in the section entitled 'Strain monitoring'. Datum readings (at week 0 in the figures) were taken 24 h after the application of repair. The repair with material S1 (Fig. 17) was depropped at week 1. This

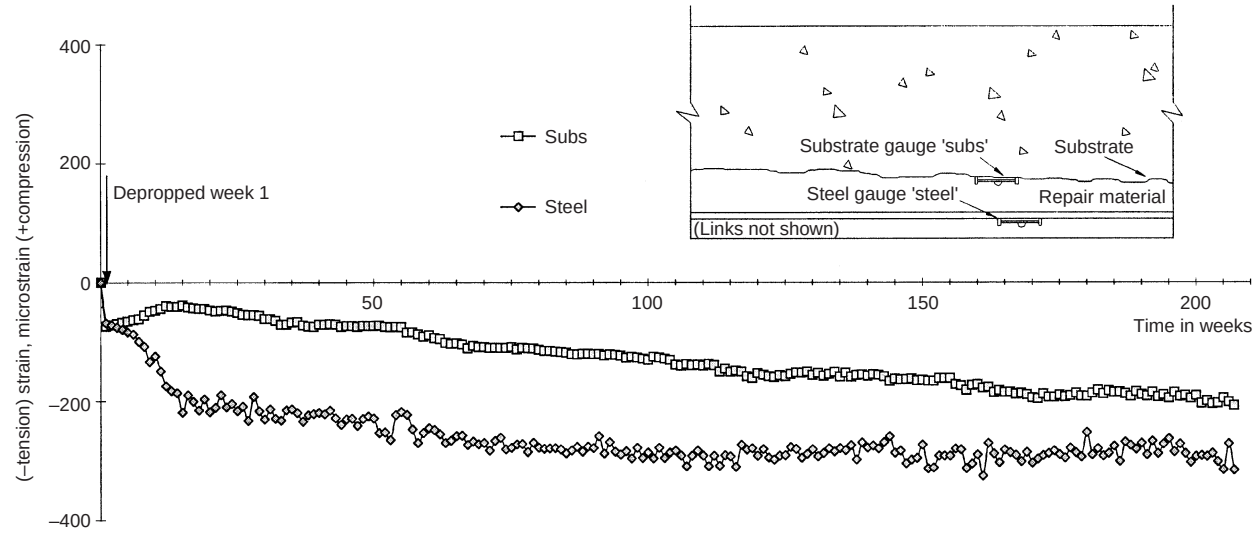

Fig. 17. Strain profiles in the portal frame beam repaired with flowing material S1, Sutherland Street bridge, propped repair, $E_{rm} > E_{sub}$

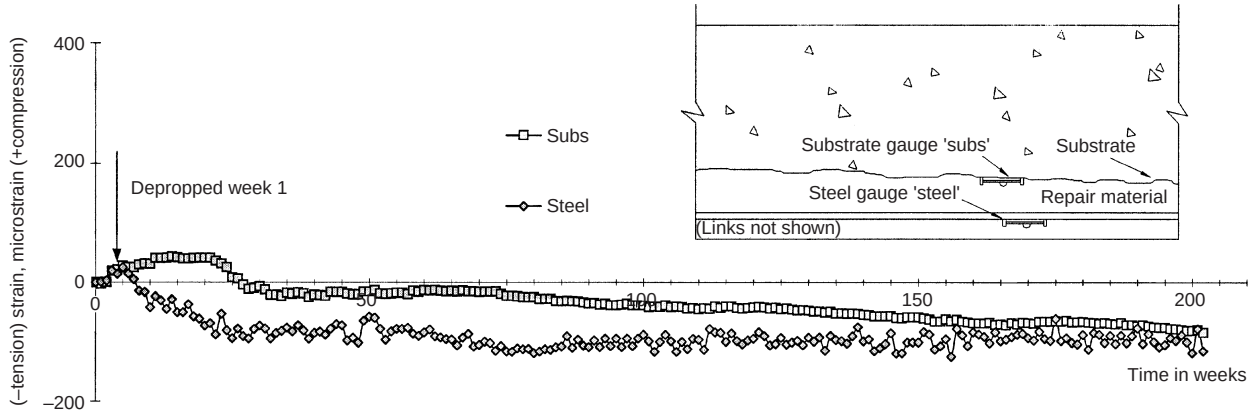

Fig. 18. Strain profiles in the portal frame beam repaired with flowing material S4, Sutherland Street bridge, propped repair, $E_{rm} > E_{sub}$

induced instantaneous tensile strains in the repair at the 'subs' gauge location and in the steel reinforcement (approximately 75 microstrain). The tensile strain in the reinforcement increased rapidly to approximately 220 microstrain at week 18. This was due to extensive cracking in the repair patch where closely spaced horizontal cracks across the width of soffit were observed. From week 18 onwards, the steel strain remained fairly constant until the end of the monitoring period. Material S1 has also been used to repair propped compression members,[13] in which case no long-term cracking was observed in the repair patch.[13] This indicates that cracking in the propped flexural repair is due to sudden load transfer upon depropping instead of long-term shrinkage effects.

The tensile strain recorded by the 'subs' gauge, upon depropping (Fig. 17), gradually decreases up to about 14 weeks. This is possibly due to the shrinkage transfer of the relatively stiffer repair material ($E_{\mathrm{rm}} > E_{\mathrm{sub}}$) to the substrate in a similar manner as was observed in bridge abutments repaired with sprayed materials.[12] In the long term, beyond 20 weeks, a gradual increase in tensile strain occurs in the repair material at the substrate interface ('subs' gauge), indicating load redistribution effects occurring in the repair patch.

The repair with material S4, Fig. 18, was depropped at week 3. Between weeks 3 and 21, the tensile strain in the steel reinforcement increases gradually, without any sudden and rapid increase as shown in Fig. 17 for material S1. This is due to material S4 remaining uncracked throughout the monitoring period. The effects of depropping are far more inconsistent in field structures compared with laboratory repairs (see next subsection) due to the greater control of depropping in the laboratory. Repairs to propped compression members also showed inconsistent and erratic long-term strain distribution due to the non-uniform load transfer caused by the depropping process.[13]

The absence of cracking in the repair patch (Fig. 18) also allows some shrinkage transfer from the higher stiffness repair material ($E_{\mathrm{rm}} > E_{\mathrm{sub}}$) to the substrate. In the long term the substrate develops tensile strain due to external load transfer; similar behaviour of load transfer has been observed in compression members.[12]

Laboratory tests, $E_{rm} < E_{sub}$. The strain profiles of the beam repaired with material G5 (Table 2), in the propped state, are presented in Fig. 19. The beam was cast in the laboratory at week −13, cured for 28 days to week −9 and loaded under service load for nine weeks (week −9 to 0). To simulate propped repair, the load was removed at week 0 and the repair patch applied. Upon hardening of the repair, at week +2, the load was reapplied (simulating depropping).

A comparison of Figs 12 and 19, representing unpropped and propped repairs, shows that the strain profiles in the substrate (compression zone) are similar in both cases (gauges Dem 1, Dem 2 and Dem 3). The strain profiles for the steel reinforcement appear similar in both cases but the magnitude of strain in the propped repair (Fig. 19) is clearly higher. This is due to the fact that upon application of load (depropping), the tensile zone (repair patch) cracked in the typical pattern of reinforced concrete beams. Such flexural cracking was not observed in the unpropped repair (Fig. 12) where effective structural interaction between the substrate and the repair patch occurred gradually with time. In the case of propped repairs, long-term interaction between the repair patch and substrate is ineffective both in beams and compression members.[13]

Conclusions

The following conclusions are based on laboratory and field monitoring of repairs under long-term service loading.

(*a*) Repair patches of high elastic modulus materials, $E_{\mathrm{rm}} > E_{\mathrm{sub}}$, provide structurally efficient repairs to the tensile zone of beams. Such repairs are less prone to restrained shrinkage cracking and are

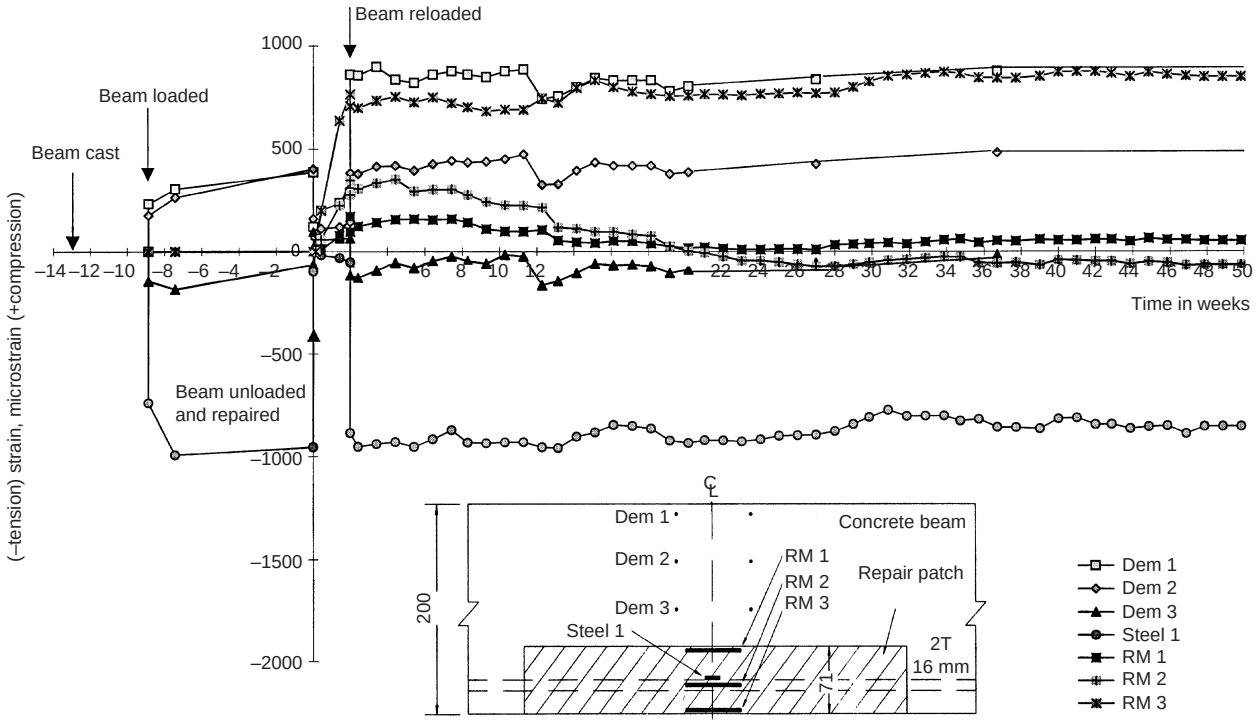

Fig. 19. Strain profiles in the beam repaired with material G5(L), $E_{rm} < E_{sub}$, propped repair

more effective in long-term load sharing with the substrate. The efficiency is greater with increasing relative stiffness within the experimental limits of this paper, $E_{sub} < E_{rm} < 1{\cdot}38E_{sub}$.

(*b*) Repairs with $E_{rm} < E_{sub}$ are generally structurally inefficient. They are prone to restrained shrinkage cracking and make little contribution to the structural capacity of the beam. This conclusion is based on test data representing repair materials of elastic modulus range $0{\cdot}41E_{sub}$–$0{\cdot}96E_{sub}$; shrinkage range 401–1100 microstrain and creep range 745–1411 microstrain.

The characteristics outlined in items (*a*) and (*b*) are clearly defined in repairs applied to unpropped structures. In propped repairs, these effects are overshadowed by the immediate effects of depropping after the repair patch has hardened. Upon depropping, the repair patch acts compositely with the beam and consequently develops a typical pattern of flexural cracking. The structural efficiency of propped repairs is inferior to unpropped repairs.

Acknowledgements

This paper is based on a LINK TIO project entitled 'Long-term Performance of Concrete Repair in Highway Structures'. The partners in the project were: Sheffield Hallam University, V. A. Crookes (Contracts) Ltd, Flexcrete Ltd, M. J. Gleeson Group plc. The contributions of all project partners, the former Department of Transport, the Highways Agency and local authorities (Nottinghamshire, Sheffield) are gratefully acknowledged.

References

1. Department of Transport. *The Performance of Concrete in Bridges: A Survey of 200 Highway Bridges*. Report by G. Maunsell and Partners, HMSO, London, 1989.
2. Department of Transport. *Materials for the Repair of Concrete Highway Structures*. DoT, London, 1986, Report No. BD27/86.
3. US Department of the Interior Bureau of Reclamation. *Standard Specifications for Repair of Concrete*. US Department of the Interior Bureau of Reclamation, Denver, Report No. M470000. 296.
4. The Concrete Society. *Patch Repair of Reinforced Concrete Subject to Reinforcement Corrosion, Model Specifications and Method of Measurement*. 1991, Technical Report No. 38, ISBN 094669137.1.
5. Wood J. G. M., King E. S. and Leek D. S. Defining the properties of concrete repair materials for effective structural applications. *Proceedings of an International Conference on Structural Faults and Repair*, London, 1989, vol. 89, p. 2.
6. Dector M. H. and Lambe R. W. New materials for concrete repair—development and testing. *The Indian Concrete Journal*, 1993, Oct., 475–480.
7. Mangat P. S. and O'Flaherty F. J. Keynote paper: Long-term performance criteria for concrete repair materials. *Proceedings of an International Congress, Creating with Concrete, Concrete Durability and Repair Technology*, University of Dundee, 6–10 September 1999.
8. Emmons P. H. and Vaysburd A. M. Performance criteria for concrete repair materials, Phase 1. Technical Report REMR-CS-470 for the US Army Corps of Engineers, US army engineers waterways equipment station (in press).

9. EMMONS P. H., VAYSBURD A. M. and VIXBURG M. S. A total system concept—necessary for improving the performance of repaired structures. *Concrete International*, 1995, Mar., 31–36.
10. EMBERSON N. K. and MAYS G. C. Significance of property mismatch in the patch repair of concrete. Part 3: Reinforced concrete members in flexure. *Magazine of Concrete Research*, 1996, **48**, No. 174, Mar., 45–47.
11. RIZZO E. M. and SOBELMAN M. B. Selection criteria for concrete repair materials. *Concrete International*, 1989, Sept., 46–49.
12. MANGAT P. S. and O'FLAHERTY F. J. Long-term performance of high stiffness repairs in highway structures. *Magazine of Concrete Research*, 1999, **51**, No. 5, Oct., 325–339.
13. MANGAT P. S. and O'FLAHERTY F. J. Serviceability characteristics of flowing repairs to propped and unpropped bridge structures. *Rilem Materials and Structures*. 1999, **32**, Nov., 663–672.
14. MANGAT P. S. and O'FLAHERTY F. J. Influence of elastic modulus on stress redistribution and cracking in repair patches. *Cement and Concrete Research* **30**, 2000, 125–136.
15. MANGAT P. S. and ELGARF M. S. Strength and serviceability of repaired reinforced concrete beams undergoing reinforcement corrosion. *Magazine of Concrete Research*, 1999, **51**, No. 2, Apr., 97–112.
16. MANGAT P. S. and ELGARF M. S. Bond characteristics of corroding reinforcement in concrete beams. *Materials and Structures*, 1999, **32**, Mar., 89–97.
17. ASAD M., BALUCH M. H. and AL-GADHIB A. H. Drying shrinkage stresses in concrete patch repair systems. *Magazine of Concrete Research*, 1997, **49**, No. 181, 283–293.
18. BLIGHT G. E., ALEXANDER M. G. and LAMBERT B. J. Structural repair of reinforced concrete portal frame. *Magazine of Concrete Research*, 1993, **45**, No. 163, 97–101.
19. CAIRNS J. Analysis of structurally repaired reinforced concrete beams. *Proceedings of a Conference on Deterioration and Repair of Reinforced Concrete in the Arabian Gulf*, October 1989.

Discussion contributions on this paper should reach the editor by 21 November 2000